Intruder states of the odd-mass $N=27$ isotones

Atsushi Yokoyama
Physics Laboratory, School of Medicine, Teikyo University, Hachioji, Tokyo 192, Japan

Hisashi Horie
Department of Physics, Tokyo Institute of Technology, Meguro-ku, Tokyo 152, Japan

(Received 13 March 1984)

Energy levels and electromagnetic properties of the $N=27$ and 28 nuclei are studied systematically in terms of the shell model within the $f_{7/2}^n+f_{7/2}^{n-1}(p_{3/2},p_{1/2},f_{5/2})^1$ configurations. The effective interactons are made up of empirical matrix elements and phenomenological potentials superposed with two and three central interactions. Least-squares fitting calculations of selected energy levels are performed to fix some of the matrix elements and the strength parameters of the potentials. It is shown that some states with a collective nature appear in ^{51}Cr and ^{53}Fe which are connected to each other by the enhanced $E2$ transitions, whereas no such states appear in ^{47}Ca and ^{49}Ti. The anomalously large $B(E2)$ values observed in the transitions between the intruder states can be reproduced very well. The hindrance of the $E2$ transitions between the intruder state and the normal $f_{7/2}^n$ state is obtained in the present model, being in qualitative agreement with the experiments. Both of the proton-neutron (p-n) interactions (1) among the $f_{7/2}$ nucleons and (2) between the $f_{7/2}$ and the other fp nucleons are very important in order to obtain proper understanding of the nuclei in this mass region.

I. INTRODUCTION

A great similarity between the sequences of the low-lying negative parity states of ^{51}Cr and ^{53}Fe has been observed.[1–4] Those states can be divided almost completely into two groups. One consists of a series with $J^\pi=\frac{7}{2}^-$, $\frac{9}{2}^-$, $\frac{11}{2}^-$, ..., which can be accounted for by the normal $f_{7/2}^n$ configurations. The other is made up of a series with $J^\pi=\frac{3}{2}^-$, $\frac{1}{2}^-$, $\frac{5}{2}^-$, ..., which cannot be explained by the $f_{7/2}^n$ model, and these states are often referred to as intruder states. The intruder states may be characterized by the strongly enhanced $E2$ transitions between the members of the same group and also by the highly hindered $E2$ transitions from the member of one group to that of the other. In terms of the Nilsson model, the intruder states are interpreted[3] as the members of a $K^\pi=\frac{1}{2}^-$ band, while the other states are assigned as the members of a $K^\pi=\frac{7}{2}^-$ band. This model works quite well in explaining the hindrance of the interband $E2$ transition as a $\Delta K=3$ forbidden transition as well as the enhancement of the intraband $E2$ transitions. From a shell-model point of view, there have been few interpretations based on systematic calculations, although it was shown[5] with the $f_{7/2}^n+f_{7/2}^{n-1}p_{3/2}$ configurations that only the $\frac{3}{2}^-$ state was predicted in the low energy region in the odd-mass $N=27$ isotones, whereas the $\frac{1}{2}^-$ and $\frac{5}{2}^-$ states were missing in the same energy region. Calculations including the one-particle excitations into all the $p_{3/2}$, $p_{1/2}$, and $f_{5/2}$ orbits were done,[6] but they were restricted to ^{53}Fe only and were not applied to ^{51}Cr. The purpose of the present paper is to show how the intruder states characterized by the enhanced $E2$ transitions do develop in the heavier mass $N=27$ isotones, ^{51}Cr and ^{53}Fe, and do not appear in the lighter mass isotones, ^{47}Ca and ^{49}Ti, by systematic calculations of the whole $N\sim28$ nuclei with the

$$f_{7/2}^n+f_{7/2}^{n-1}(p_{3/2},p_{1/2},f_{5/2})^1$$

configurations.

Recently, several authors[6–9] performed shell-model calculations in this mass region by allowing one-particle excitations from the $f_{7/2}$ to the other three fp orbits. The renormalized G-matrix elements[10] deduced from realistic nucleon-nucleon interactions were used together with empirical matrix elements. The monopole corrections[11] were added to the diagonal G-matrix elements in their analysis. Johnstone and Benson[7] tried to understand intruder states generated by the one-particle excited configurations, but they neglected configuration mixing between two different configurations. Styczen *et al.*[8] took account of the configuration mixing by introducing the off-diagonal G-matrix elements into the effective interactions obtained in Ref. 7 with the slight modification of the diagonal matrix elements. The Utrecht group[6,9] attempted to introduce "scale factors" by which the G-matrix elements were multiplied, and they determined these factors by least-squares fitting calculations. It turned out, however, that the scale factors varied considerably in going from one nucleus to the other. Therefore, one cannot expect that the effective interactions which explain one particular nucleus (or isotope) can be applied successfully to the other nuclei. Mooy and Glaudemans[9] have recently made a calculation of $A=52$–60 nuclei by introducing mass independent scale factors. The scale factors in this case are not uniform for all the two-body matrix elements but are defined individually for each specific form of the matrix

elements, i.e., they depend on the orbital angular momentum of the two interacting particles. Some of the scale factors have been determined in the least-squares fitting calculations, and it turns out that the fitted values strongly depend on the form of the two-body matrix elements, suggesting that the phenomenologically adopted effective interactions should deviate considerably from the original G-matrix elements. Thus, the parametrization based upon the G-matrix elements with monopole corrections seems to be still unsatisfactory to provide an appropriate description of the effective interactions for the

$$f_{7/2}^{n}+f_{7/2}^{n-1}(p_{3/2},p_{1/2},f_{5/2})^{1}$$

space. The surface delta interaction (SDI) was also tried[6,9] instead of the G-matrix elements, but the results were even worse than those with the realistic interactions, especially in the $M1$ properties. It is therefore needed to obtain the effective interactions relevant to the assumed model space in order to perform systematic calculations of the whole nuclei in the $N\sim 28$ region. Since we do not have enough experimental data available to make an empirical determination of all the matrix elements completely, we have to impose some assumptions on the effective interactions. In the present work, we introduce partly empirical matrix elements and partly phenomenological potentials. By adjusting the matrix elements and the strength parameters of the potentials to reproduce selected energy levels in the least-squares fitting calculations, we try to obtain the effective interactions relevant to the model space of the

$$f_{7/2}^{n}+f_{7/2}^{n-1}(p_{3/2},p_{1/2},f_{5/2})^{1},$$

configurations.

In Sec. II, we describe the assumptions imposed on the effective interactions and also present the results of the least-squares fitting calculations. The properties of the $N=27$ nuclei are discussed in Sec. III. Concluding remarks are presented in Sec. IV.

II. EFFECTIVE INTERACTIONS

A. Parametrization

If one- and two-body forces are assumed for the effective interactions in the model space of the

$$f_{7/2}^{n}+f_{7/2}^{n-1}(p_{3/2},p_{1/2},f_{5/2})^{1}$$

configurations, four single-particle energies and 60 two-body matrix elements are needed in the calculation of the shell-model Hamiltonian. In order to reduce ambiguities on the effective interactions, an empirical approach is tried in our calculations. We cannot hope, however, that all the single-particle energies and two-body matrix elements are treated as independent adjustable parameters and are determined unambiguously by the least-squares fitting procedure, since the number of adjustable parameters is so large compared with that of available experimental data. Therefore, we are obliged to reduce the number of parameters to make the least-squares fitting calculations manageable in size, by introducing partly phenomenological potentials to calculate some of the two-body matrix elements. For this purpose, we classify the two-body matrix elements into three groups: (i) $\langle f_{7/2}^{2}\,|\,V\,|\,f_{7/2}^{2}\rangle_{TJ}$, (ii) $\langle f_{7/2}j\,|\,V\,|\,f_{7/2}j'\rangle_{TJ}$, and (iii) $\langle f_{7/2}^{2}\,|\,V\,|\,f_{7/2}j\rangle_{TJ}$, where j and j' represent one of the $p_{3/2}$, $p_{1/2}$, and $f_{5/2}$ orbits, and T and J denote the isospin and the total angular momentum, respectively, resulting from the coupling of the two interacting particles. Since the eight matrix elements of type (i) play significant roles in reproducing both binding and excitation energies, we do not specify the form of these matrix elements, and they are treated as adjustable parameters in the least-squares fitting calculations.

The average interaction energies for type (ii) interactions are defined by

$$V(f_{7/2}j)_{T}=\frac{1}{8(2j+1)}\sum_{J}(2J+1)\langle f_{7/2}j\,|\,V\,|\,f_{7/2}j\rangle_{TJ}\ ,$$

and can be estimated empirically by using the single-neutron energies extracted from ^{41}Ca, ^{49}Ca, and ^{57}Ni. The average interaction energies for the neutron-neutron (n-n) interactions ($T=1$) are weakly repulsive and do not depend on the orbit j so much, whereas those for the proton-neutron (p-n) interactions ($T=1$ plus $T=0$) are strongly attractive and depend heavily on the orbit j. It has been pointed out[12] that only central interactions do not work very well to reproduce the properties of the p-n interactions, particularly the difference between those for $j=p_{3/2}$ and $p_{1/2}$. The noncentral interactions such as the tensor force and the spin-orbit force might play a role in the p-n interactions, but it is quite difficult to determine all the parameters for each component unambiguously by the least-squares fitting calculation. Therefore, for the p-n matrix elements of type (ii), we employ the empirical p-n interactions obtained by Horie and Ogawa[12] in the analysis of the $N=29$ isotones. The p-n matrix elements for type (ii) are given by

$$V_{\rm pn}=(V_{T=1}+V_{T=0})/2\ ,$$

and thus either the $T=1$ or $T=0$ part of the type (ii) matrix elements remains unknown. In the present calculations, we assume phenomenological two-body potentials to calculate the $T=1$ matrix elements of type (ii). Since nothing has yet been known on the effective interactions of type (iii), the phenomenological potentials are also assumed to calculate both of the $T=1$ and $T=0$ matrix elements.

The phenomenological potentials assumed in calculating some of the matrix elements are generated by superposing central interactions of the delta function, Yukawa, and monopole types. The noncentral interactions are not adopted for the sake of simplicity. In the singlet-triplet and even-odd representation, the central interaction is parametrized by

$$V(r)=(V_{\rm SO}P^{\rm SO}+V_{\rm TE}P^{\rm TE}+V_{\rm SE}P^{\rm SE}+V_{\rm TO}P^{\rm TO})f(r)\ .$$

Here, $P^{\rm SO}$, $P^{\rm TE}$, $P^{\rm SE}$, and $P^{\rm TO}$ are projection operators for the singlet-odd, triplet-even, singlet-even, and triplet-odd states, respectively. The radial dependence is denoted by $f(r)$, and its explicit form is given by $\delta(r)/r^{2}$ for the delta function, by $\exp(-\mu r)/\mu r$ for the Yukawa, and by 1 for

the monopole types, where $1/\mu=1.414$ fm (one-pion exchange range). The radial integrals for the two-body interactions are evaluated by using the harmonic oscillator wave functions with the oscillator constant

$$\nu=m\omega/\hbar=0.96\times A^{-1/3}\ \text{fm}^{-2}\ ,$$

where $A=52$, and we assume that the radial functions are positive near the origin. The integration is performed in momentum space by applying a method which uses a Fourier transform.[13]

The monopole interaction gives nonvanishing contributions for the radial matrix elements which are diagonal with respect to the orbital angular momentum. Since the spin exchange mixture is assumed for any central interaction, the matrix elements, $\langle f_{7/2}^2 \mid V \mid f_{7/2}f_{5/2}\rangle_{TJ}$, for the monopole interaction do not necessarily vanish, even though they are nondiagonal in the *jj* coupling form. The contributions from the even and odd states are not independent, however. They are the same size and have the opposite sign. In calculating the $T=0$ matrix elements, singlet-odd and triplet-even components contribute, and we choose only the triplet-even strength as an adjustable parameter for the $T=0$ monopole interaction. For the $T=1$ monopole interaction, we can still treat the singlet-even and the triplet-odd strength as independent parameters, since in calculating the type (ii) matrix elements they are totally independent.

The $f_{7/2}$ and $p_{3/2}$ single-particle energies are treated as adjustable parameters, whereas the $p_{1/2}$ and $f_{5/2}$ ones are fixed so as to reproduce the observed single-particle spectra of ^{49}Ca:

$$\text{BE}(\tfrac{1}{2}^-)-\text{BE}(\tfrac{3}{2}^-)=2.028\ \text{MeV}$$

and

$$\text{BE}(\tfrac{5}{2}^-)-\text{BE}(\tfrac{3}{2}^-)=3.958\ \text{MeV (Ref. 12)}\ ,$$

where BE(J^π) denoted the binding energies of the states in ^{49}Ca.

Four kinds of the phenomenological potentials are assumed in the least-squares fitting calculations in order to check the radial dependence of the short range interaction. Since the range of the long range interaction is roughly the nuclear size, we adopt only the monopole interaction as the long range interaction. They are given by: *A*, delta plus monopole; *B*, even Yukawa plus monopole; *C*, Yukawa plus monopole; *D*, delta plus Yukawa plus monopole. In the potential *B*, even Yukawa means the interaction with even components only.

B. Least-squares fitting calculations

The effective interaction parameters are determined by fitting the 72 experimental data selected from the $N=27$ and 28 nuclei. In selecting the fitting data, we follow the previous calculation[5] of the $f_{7/2}^n+f_{7/2}^{n-1}p_{3/2}$ configurations with the 63 experimental data, and we further add 9 data which are newly known. The binding energies[14] are evaluated relative to that of ^{56}Ni and the Coulomb energies are excluded from the binding energies (BE) by using the Coulomb displacement energies.[15] The binding energies are used only for the ground states and the excited states are fitted relative to their own ground states. The energy levels which are adjusted in the least-squares fitting calculation are tabulated in Table I. Only the result with the potential *D* is shown in this table, however, since there are no significant differences among the results with the various potentials. All the fitted parameters are given in Table II, and their properties are summarized as follows:

(1) When the Yukawa radial shape is used for the short-range interaction instead of the delta function, only a slight improvement is obtained. The odd component of the Yukawa radial shape does not play an important role in improving the quality of the least-squares fitting calculation.

(2) Both even and odd components of the monopole interaction are indispensible in fitting the $T=1$ interactions. It turns out that these components take the different values as the result of the least-squares fitting calculations. This means that the spin exchange force in the monopole interaction is very important, whereas the spin exchange mixture is included neither in the monopole part of the modified surface delta interaction nor in the monopole part added to the *G*-matrix elements.

(3) The potential *D* with the three different ranges does not improve the quality of the least-squares fitting calculation. The assumption of the two-range central interactions seems to work quite well as has been pointed out by Schiffer and True.[17]

In the following calculations, we will use the potential *D* which gives the smallest chi-squared value.

III. RESULTS AND DISCUSSIONS

By using the matrix elements of the effective interaction *D* and the single-particle energies obtained in Sec. II, we have calculated energy levels, spectroscopic factors, and electromagnetic transitions and moments of the $N\sim28$ nuclei. In the present work, we concentrate on a detailed description of the $N=27$ isotones. The other topics such as Gamow-Teller—type beta decay properties will be published in a subsequent paper. In calculating the electromagnetic transition matrix elements, we use the harmonic oscillator wave functions with the oscillator constant $\nu=0.96\times A^{-1/3}$ fm^{-2}, where A is the mass number of a nucleus. The effective charges $e_p=1.5e$ and $e_n=1.0e$ and the free nucleon g factors are assumed for the calculation of the $E2$ and $M1$ matrix elements, although a slight change is tried in some cases. The spectroscopic strength G_{lj} for the single-nucleon transfer reactions is defined by

$$G_{lj}=\frac{1}{2J_i+1}\mid\langle T_fT_{z_f}J_f\mid\mid a^\dagger(\tfrac{1}{2}t_zlj)\mid\mid T_iT_{z_i}J_i\rangle\mid^2\ .$$

A. Energy levels

Figures 1 and 2 show the calculated and observed[1–4] energy spectra of ^{51}Cr and ^{53}Fe, respectively. The significant feature in the present calculations is that the $\frac{1}{2}^-$ and $\frac{5}{2}^-$ states appear in the low energy region in addition to

the $\frac{3}{2}^-$ states, in contrast to the previous calculations[5] with the $p_{3/2}$ orbit only. The calculated excitation energies are, however, still higher by about 0.5 MeV than the experimental ones. The resultant wave functions of these levels consist mainly of several

$$|\Psi^{N=26}(J'=0^+_{\text{gnd}},2^+_1)\times\nu j\rangle$$

components, showing deviation from the weak coupling

TABLE I. Experimental (Refs. 1, 2, 5, 14, 15, and 16) and calculated energy levels adopted in the least-squares fitting calculation with the potential *D*. Binding energies relative to that of ^{56}Ni are used for the ground states, while excitation energies are used for the excited states. Both of them are given in MeV.

Nucleus	Spin	Experiment	Calculation	Nucleus	Spin	Experiment	Calculation
^{47}Ca	$\frac{7}{2}^-$	143.546	143.799	^{51}V	$\frac{7}{2}^-$	81.545	81.371
	$\frac{3}{2}^-$	2.016	2.058		$\frac{3}{2}^-$	0.929	1.106
					$\frac{3}{2}^-$	2.409	2.592
^{48}Sc	6^+	127.025	127.109		$\frac{5}{2}^-$	0.320	0.311
	1^+	2.520	2.737		$\frac{5}{2}^-$	3.085	3.187
	2^+	1.145	1.209		$\frac{9}{2}^-$	1.813	1.865
	2^+	2.275	2.080		$\frac{11}{2}^-$	1.609	1.620
	3^+	0.623	0.540		$\frac{11}{2}^-$	3.614	3.397
	3^+	2.190	2.284		$\frac{13}{2}^-$	3.387	3.209
	4^+	0.253	0.229		$\frac{15}{2}^-$	2.699	2.854
	4^+	2.619	2.647		$\frac{15}{2}^-$	3.874	3.743
	5^+	0.133	0.056				
	5^+	2.064	1.847	^{52}Cr	0^+	62.974	63.002
	7^+	1.096	1.325		2^+	1.434	1.452
					2^+	2.965	3.150
^{49}Ti	$\frac{7}{2}^-$	108.267	108.405		2^+	3.772	3.783
	$\frac{3}{2}^-$	1.382	1.306		3^+	3.472	3.427
	$\frac{3}{2}^-$	1.582	1.632		4^+	2.370	2.371
					4^+	2.768	2.533
					4^+	3.414	3.415
					5^+	3.617	3.522
					5^+	4.015	4.203
					6^+	3.114	2.970
^{53}Fe	$\frac{7}{2}^-$	43.924	43.932		8^+	4.750	4.803
	$\frac{9}{2}^-$	1.328	1.418	^{53}Mn	$\frac{7}{2}^-$	48.065	48.007
	$\frac{11}{2}^-$	2.339	2.348		$\frac{1}{2}^-$	2.672	2.521
	$\frac{13}{2}^-$	3.176	3.278		$\frac{3}{2}^-$	1.289	1.158
	$\frac{15}{2}^-$	3.463	3.302		$\frac{3}{2}^-$	2.407	2.552
	$\frac{19}{2}^-$	3.041	3.119		$\frac{5}{2}^-$	0.378	0.269
					$\frac{9}{2}^-$	1.621	1.782
					$\frac{11}{2}^-$	1.441	1.594
					$\frac{11}{2}^-$	2.697	2.860
					$\frac{13}{2}^-$	2.564	2.761
^{49}Sc	$\frac{7}{2}^-$	116.897	116.570		$\frac{13}{2}^-$	3.426	3.555
	$\frac{3}{2}^-$	3.084	2.769		$\frac{15}{2}^-$	2.693	2.699
					$\frac{15}{2}^-$	3.440	3.602
				^{54}Fe	0^+	30.542	30.608
					2^+	1.408	1.390
^{50}Ti	0^+	97.319	97.193		4^+	2.539	2.436
	2^+	1.554	1.518		6^+	2.948	2.806
	2^+	4.184	4.061				
	4^+	2.677	2.643	^{55}Co	$\frac{7}{2}^-$	16.519	16.427
	4^+	4.158	3.860		$\frac{3}{2}^-$	2.186	2.199
	6^+	3.201	3.131		$\frac{3}{2}^-$	2.564	2.855

TABLE II. Values of the two-body matrix elements, the depth parameters of the various potentials, and the single-particle energies determined by the least-squares fitting calculations (in MeV). The χ^2 is defined by $\chi^2=\sum_{i=1}^{m}(E_i^{\rm cal}-E_i^{\rm expt})^2$, and the rms deviation is given by $[\chi^2/(m-n)]^{1/2}$, where m is the number of experimental data and n is the number of parameters. For the parameters of the delta and the Yukawa functions, the weight is assumed to be 100 so as to make the sensitivity of the parameters roughly equal to that of the others. The weight for the other parameters and for the fitting data is assumed to be 1.

		A	*B*	*C*	*D*
$\langle f_{7/2}^2 \mid V \mid f_{7/2}^2 \rangle_J$	$J=1$	−2.0368	−2.0224	−2.0668	−2.0095
	$J=3$	−0.5922	−0.6397	−0.6568	−0.6226
	$J=5$	−0.4311	−0.4525	−0.4581	−0.4681
	$J=7$	−2.1611	−2.1411	−2.1248	−2.1440
	$J=0$	−2.6067	−2.5945	−2.6143	−2.5987
	$J=2$	−1.0859	−1.0366	−1.0208	−1.0552
	$J=4$	0.0286	0.0484	0.0614	0.0771
	$J=6$	0.5203	0.4910	0.4806	0.4734
$V_{\rm TE}$(delta)		−17.189			−41.818
$V_{\rm SO}$(Yukawa)				−63.238	−108.93
$V_{\rm TE}$(Yukawa)			−21.228	−20.786	24.896
$V_{\rm TE}$(monopole)		−0.6689	−0.3617	−1.6285	−3.0244
$V_{\rm SE}$(delta)		−45.273			15.410
$V_{\rm SE}$(Yukawa)			−49.977	−50.073	−65.737
$V_{\rm TO}$(Yukawa)				0.540	1.144
$V_{\rm SE}$(monopole)		0.1348	0.9141	0.9033	1.1350
$V_{\rm TO}$(monopole)		0.4655	0.4616	0.4505	0.4372
$\epsilon_{7/2}$		−10.4747	−10.4625	−10.4648	−10.4387
$\epsilon_{3/2}$		−6.9028	−6.7533	−6.7129	−6.7289
χ^2 (in MeV^2)		1.519	1.468	1.464	1.449
rms deviation (in keV)		163	160	163	165

picture. Here, $\Psi^{N=26}$ denotes the wave functions of the even-even $N=26$ nuclei, calculated within the $f_{7/2}^n$ configurations, and j denotes the $p_{3/2}$, $p_{1/2}$, and $f_{5/2}$ orbits. The levels connected with these low-spin intruder states by the relatively large $E2$ transition strengths are also shown in these figures, and it turns out that the sequence of such levels continues up to $J^\pi=\frac{33}{2}^-$ in ^{51}Cr, while it terminates at $J^\pi=\frac{13}{2}^-$ in ^{53}Fe. These levels are all generated predominantly by the neutron excitations from the $f_{7/2}$ to the other fp orbits. Deviation from the weak coupling picture is also found, and the admixture of various components in the wave functions is essential to obtain the coherent sum of the $E2$ matrix elements between the intruder states. In the previous calculations[5] with the $p_{3/2}$ orbit only, there appeared some intruder states connected to each other by the appreciable $E2$ transitions. The transition rates are, however, not so much enhanced, and then, the sequence is not so clear, as compared with the present calculations. Therefore, the inclusion of all the $p_{3/2}$, $p_{1/2}$, and $f_{5/2}$ orbitals is very important to obtain the enhancement of the $E2$ rates between the intruder states.

High-spin yrast states, which may be populated by heavy-ion reaction experiments, are also presented in Figs. 1 and 2. They are generated predominantly by the one-particle excited configurations, and it turns out that the neutron excitations are dominant in ^{51}Cr, whereas in ^{53}Fe both the proton and neutron excitations contribute to the $J^\pi\leqq\frac{27}{2}^-$ states. The $f_{7/2}^{n-1}p_{3/2}$ components are not necessarily the major ones in the wave functions and all the excitations into the three fp orbits are important, in contrast to the previous calculations.[5] Although the present calculations predict several branches for the deexcitation processes of those high-spin states, there are relatively strong decay modes before decaying into the $f_{7/2}^n$ yrast states. There are two sequences in ^{51}Cr. One is $\frac{33}{2}^-\rightarrow\frac{29}{2}^-\rightarrow\frac{25}{2}^-\rightarrow\frac{23}{2}^-(1)$, and the other is $\frac{31}{2}^-\rightarrow\frac{27}{2}^-\rightarrow\frac{23}{2}^-(2)\rightarrow\frac{21}{2}^-(1)$. The calculated branching ratio for the $\frac{25}{2}^-\rightarrow\frac{23}{2}^-(1)$ transition is 31%, and that for the $\frac{23}{2}^-(2)\rightarrow\frac{21}{2}^-(1)$ is 35%. The $\frac{25}{2}^-$ state can also decay into the $\frac{23}{2}^-(2)$ state with a 31% branch. The other branches are relatively small and therefore the levels with $J^\pi\leqq\frac{19}{2}^-$ below 6 MeV in ^{51}Cr might be weakly populated or could not be seen in the deexcitation processes. In ^{53}Fe, the present calculation predicts that the main cascade is $\frac{29}{2}^-\rightarrow\frac{27}{2}^-\rightarrow\frac{25}{2}^-\rightarrow\frac{21}{2}^-$, and then the $\frac{21}{2}^-$ state decays mostly into the isomeric $\frac{19}{2}^-$ state by the $E2$ transition [$B(E2)=21\ e^2\,\mathrm{fm}^4$]. The $\frac{23}{2}^-$ state decays into the isomeric $\frac{19}{2}^-$ state with a 90% branch. Thus, the

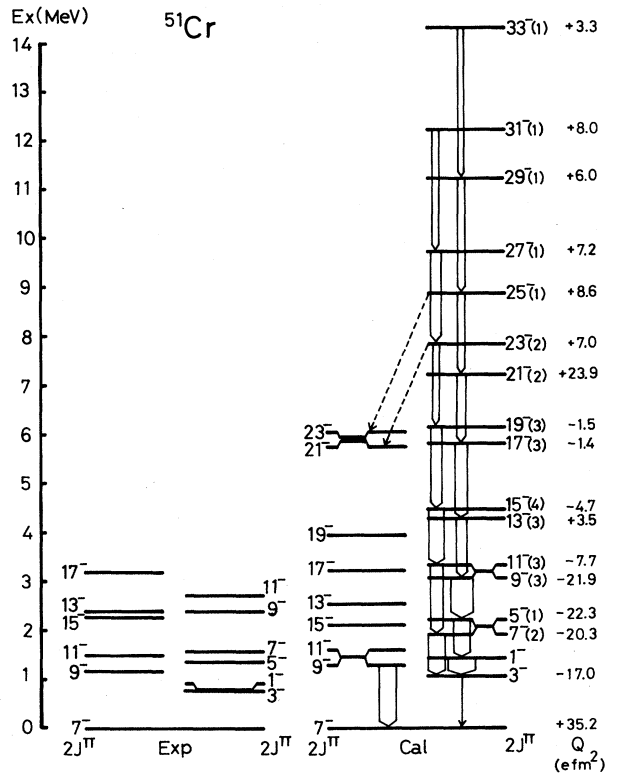

FIG. 1. Calculated and experimental (Refs. 1, 3, and 4) energy spectra of ^{51}Cr. In each spectrum the $f^n_{7/2}$ levels are shown on the left-hand side (lhs), and the intruder states are on the right-hand side (rhs). The levels connected with the low-spin intruder states by the relatively large $E2$ transition rates are shown, and the $B(E2)$ values are presented by the arrows, being proportional to the width. The number given in the parentheses is that of the eigenstate counted from the lowest one with the certain angular momentum J. The Q moments in e fm^2, calculated with $e_p=1.5e$ and $e_n=1.0e$, are shown on the rhs of the levels. The relatively strong transitions from the high-spin yrast states to the $f^n_{7/2}$ states are shown by the arrow with the dashed line.

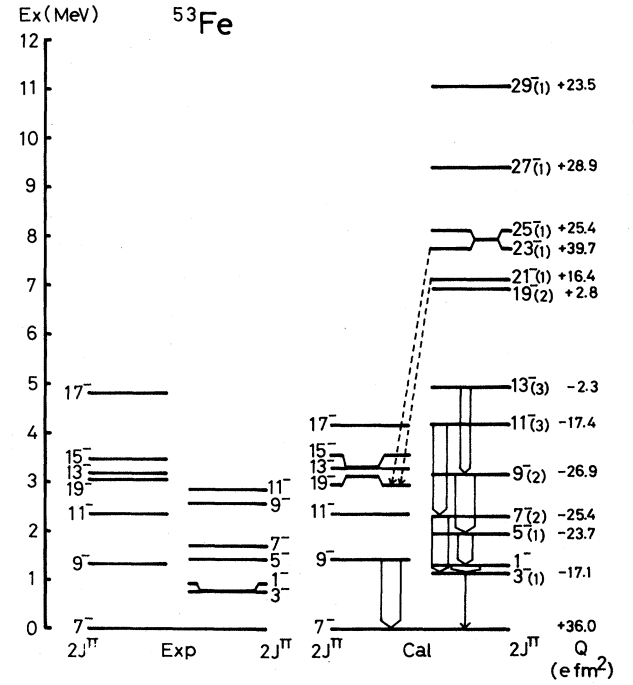

FIG. 2. Calculated and experimental (Refs. 2 and 4) energy spectra of ^{53}Fe. See the caption to Fig. 1.

$J^{\pi} \leqq \frac{19}{2}^-$ states below 7 MeV in ^{53}Fe could not be seen in the deexcitation processes.

B. $E2$ properties

The $E2$ rates between the $f^n_{7/2}$ levels can be reproduced very well by using the effective charges $e_p=1.5e$ and $e_n=1.0e$. For example, we obtain $B(E2)=161$ e^2fm^4 for the $\frac{9}{2}^-(1)\rightarrow\frac{7}{2}^-_{gnd}$ transition in ^{51}Cr, which is comparable with the experimental value[4] 121^{+29}_{-35} e^2fm^4. On the other hand, the $E2$ rates between the intruder states are underestimated by about a factor of 2, as long as the same effective charges are assumed. Since the intruder states are generated mainly by the $|\Psi^{N=26}(f^{n-1}_{7/2}\alpha'T'J')\times\nu j\rangle$ states, we try to extract the effective charges for the intruder states so as to reproduce the $B(E2;2^+_1\rightarrow 0^+_{gnd})$ in the neighboring even-even $N=26$ nuclei within the $f^{n-1}_{7/2}$ configurations. We increase only the isoscalar part of the effective charges, and thus we have $e_p=2.0e$ and $e_n=1.5e$. The calculated $B(E2)$ values in ^{51}Cr with them are 315 e^2fm^4 for the $\frac{7}{2}^-(2)\rightarrow\frac{3}{2}^-(1)$, 411 e^2fm^4 for the $\frac{9}{2}^-(3)\rightarrow\frac{5}{2}^-(1)$, and 311 e^2fm^4 for the $\frac{5}{2}^-(1)\rightarrow\frac{1}{2}^-(1)$ transitions. They all are consistent with the experimental values[4] 320^{+170}_{-150}, 320^{+110}_{-80}, and 240^{+140}_{-90} e^2fm^4, respectively. In ^{53}Fe, we obtain 318 e^2fm^4 for the $\frac{7}{2}^-(2)\rightarrow\frac{3}{2}^-(1)$, 373 e^2fm^4 for the $\frac{9}{2}^-(2)\rightarrow\frac{5}{2}^-(1)$, and 287 e^2fm^4 for the $\frac{5}{2}^-(1)\rightarrow\frac{1}{2}^-(1)$ transitions, which are comparable with the experimental values[4] 510^{+510}_{-310}, 250^{+130}_{-120}, and 380^{+140}_{-90} e^2fm^4, respectively.

Recent experiments of Kishimoto *et al.*[4] suggest that in ^{51}Cr the observed $\frac{11}{2}^-(2)$ level is a candidate for a member of the $K^{\pi}=\frac{1}{2}^-$ band, since the observed $E2$ transition rates from the $\frac{11}{2}^-(2)$ to the $\frac{7}{2}^-(2)$ level is 600^{+680}_{-400} e^2fm^4 and is quite large. It is also suggested in their experiments that in ^{53}Fe, on the other hand, the observed $\frac{11}{2}^-(2)$ level decays into the $\frac{7}{2}^-$ ground state with $B(E2)=50^{+50}_{-20}$ e^2fm^4, and it cannot be considered as a member of the $K^{\pi}=\frac{1}{2}^-$ band. The present calculation predicts that both in ^{51}Cr and ^{53}Fe the $\frac{11}{2}^-(3)$ levels are generated almost purely by the neutron excitations and are connected to the $\frac{7}{2}^-(2)$ levels by the strong $E2$ transition strengths. The calculated $E2$ rates from the $\frac{11}{2}^-(3)$ to the $\frac{7}{2}^-(2)$ levels are 242 e^2fm^4 in ^{51}Cr and 268 e^2fm^4 in ^{53}Fe, where $e_p=2.0e$ and $e_n=1.5e$ are assumed. If one considers that the calculated $\frac{11}{2}^-(2)$ level in ^{51}Cr is generated mostly by the $f^{11}_{7/2}$ configuration and that the excitation energies of the intruder states are estimated systematically higher by about 0.5 MeV, then it is plausible to interpret that the calculated second and third $\frac{11}{2}^-$ lev-

els in ^{51}Cr are interchanged by some effect not taken into account in the present model, and the calculated $\frac{11}{2}^-(3)$ level corresponds to the observed $\frac{11}{2}^-(2)$ one. On the other hand, in ^{53}Fe the calculated $\frac{11}{2}^-(2)$ level is composed of both proton and neutron excited configurations. Since both the second and third excited $\frac{11}{2}^-$ levels in ^{53}Fe are generated by the one-particle excitations, the relative order may not be changed. The calculated $E2$ rate from the $\frac{11}{2}^-(2)$ to the $\frac{7}{2}^-$ ground state is 29 e^2fm^4 (with $e_p=1.5e$ and $e_n=1.0e$) or 56 e^2fm^4 (with $e_p=2.0e$ and $e_n=1.5e$), which is not inconsistent with the observed one, 50^{+50}_{-20} e^2fm^4. It seems therefore that in ^{53}Fe the calculated $\frac{11}{2}^-(2)$ level corresponds to the observed $\frac{11}{2}^-(2)$ level. It would be very interesting to observe the third excited $\frac{11}{2}^-$ level in ^{53}Fe, which is expected theoretically to be slightly higher (300 keV) than the $\frac{11}{2}^-(2)$ level and to be connected to the $\frac{7}{2}^-(2)$ level by the strong $E2$ transition.

Calculated and experimental $E2$ transition rates and the spectroscopic strengths concerning the low-lying $\frac{3}{2}^-$ states of the $N=27$ isotones are summarized in Table III. The striking feature is that the $E2$ transition rates from the $\frac{3}{2}^-(1)$ to the $\frac{7}{2}^-$ ground states in ^{47}Ca, ^{51}Cr, and ^{53}Fe are strongly hindered, whereas that in ^{49}Ti is not hindered. It is also interesting to note that the $\frac{3}{2}^-(1)$ states in ^{47}Ca, ^{49}Ti, and ^{51}Cr are populated strongly by single-neutron stripping reactions. Although the hindrance of the $E2$ transitions is interpreted in terms of the Nilsson model as a $\Delta K=3$ forbidden transition, as mentioned already, it would be quite interesting to see how the shell model describes the $E2$ transition rates together with the spectroscopic factors systematically. It is shown in Table III that the qualitative features can be reproduced very well by the shell model, and the two calculations with the

$$f^n_{7/2}+f^{n-1}_{7/2}p_{3/2}$$

and the

$$f^n_{7/2}+f^{n-1}_{7/2}(p_{3/2},p_{1/2},f_{5/2})^1$$

configurations give almost the same results. The following three basis functions are the main components in the low-lying $\frac{3}{2}^-$ state wave functions:

$$|1\rangle=|f^{n-1}_{7/2}(0^+_{\rm gnd})\times\nu p_{3/2}\rangle\ ,$$

$$|2\rangle=|f^{n-1}_{7/2}(2^+_1)\times\nu p_{3/2}\rangle\ ,$$

and

$$|3\rangle=|f^n_{7/2}\rangle\ .$$

This is the common feature in both calculations, and this explains why the two calculations give almost the same results. The hindrance of the $E2$ transitions comes from the cancellation of the $E2$ matrix element from $|1\rangle$ to the ground state and that from $|2\rangle$ to the ground state. The coherent sum of these two $E2$ matrix elements should occur in some state which is orthogonal to the state producing the cancellation of the $E2$ matrix elements. Such a component is contained very much in the $\frac{3}{2}^-(2)$ states in ^{47}Ca and ^{53}Fe, and this explains the enhancement of the $E2$ transitions from the $\frac{3}{2}^-(2)$ to the ground states in these two nuclei. For the other transitions, the third components $|3\rangle$, inducing significant contributions to the $E2$ matrix elements into the ground states, play a rather complicated role. It should be noticed that the deviation from the weak coupling picture is

TABLE III. Systematics of the low-lying $\frac{3}{2}^-$ states of the $N=27$ isotones. Excitation energies, spectroscopic strengths G_{lj} for the $l_n=1$ transfer reactions, and $E2$ transition strengths from the $\frac{3}{2}^-$ states to the $\frac{7}{2}^-$ ground states are calculated and compared with experiments. The effective charges, $e_p=1.5e$ and $e_n=1.0e$, are assumed. Calculation I; $f^n_{7/2}+f^{n-1}_{7/2}p_{3/2}$ configurations (from Ref. 5). Calculation II; $f^n_{7/2}+f^{n-1}_{7/2}(p_{3/2},p_{1/2},f_{5/2})^1$ configurations (present calculation).

		Calculation I			Experiment			Calculation II		
Nucleus	No. of $\frac{3}{2}^-$ level	E (MeV)	G	$B(E2)$ (e^2fm^4)	E (MeV)	G	$B(E2)$ (e^2fm^4)	E (MeV)	G	$B(E2)$ (e^2fm^4)
^{47}Ca	1	2.066	3.70	8.2	2.016	3.6[a]	<3[d]	2.058	3.80	7.3
	2	3.520	0.30	26.8	3.297	≤ 0.07		3.113	0.17	25.9
^{49}Ti	1	1.361	1.73	90.3	1.382	1.87[b]	33.7 ± 4.5[e]	1.306	0.97	108.5
	2	1.636	1.02	27.2	1.585	0.06	$53.7^{+95.5}_{-22.6}$[e]	1.632	1.92	9.8
	3	3.511	0.44	0.0	3.260	0.63		3.051	0.52	8.3
^{51}Cr	1	1.119	2.63	16.2	0.749	1.45[c]	0.327 ± 0.001[f]	1.058	2.50	10.7
	2	1.998	0.03	85.3	1.899	0.64	60^{+13}_{-10}[g] 90^{+42}_{-21}[h]	1.859	0.01	89.7
	3	2.747	0.19	0.0	2.892	0.37		2.545	0.14	2.3
^{53}Fe	1	1.188		6.7	0.741		0.040 ± 0.001[i]	1.135		3.9
	2	2.823		56.8	2.043		67 ± 15[j]	2.416		42.7
	3	3.840		0.5				3.445		5.9

[a]From Ref. 18.
[b]From Ref. 19.
[c]From Ref. 1.
[d]From Ref. 20.
[e]From Ref. 21.
[f]From Ref. 22.
[g]From Ref. 3.
[h]From Ref. 23.
[i]From Ref. 24.
[j]From Ref. 25.

essential to cause the interference of the $E2$ matrix elements.

C. Simple interpretation of systematics of the intruder states

The reason why the sequence of the low-lying intruder states in ^{53}Fe terminates at $J^\pi=\frac{13}{2}^-$ may be attributed to the p-n interactions (1) among the $f_{7/2}$ nucleons and (2) between the $f_{7/2}$ and the other fp nucleons. In spite of the considerable deviation from the weak coupling picture, it is still instructive to use the weak coupling basis functions $|\Psi(f^n_{7/2}{}^{-1}\alpha'T'J')\times j;\alpha TJ\rangle$ in order to obtain a qualitative interpretation of the intruder states. Let us first examine the diagonal energies of these basis functions, to which the interactions among the $f_{7/2}$ nucleons are very sensitive. In ^{51}Cr, the basis states with $T'=T-\frac{1}{2}=1$ are much lower in energy than those with $T'=T+\frac{1}{2}=2$ for any J' and J, and then the intruder states generated by the $T'=1$ components can develop up to the maximum spin $\frac{33}{2}$. In ^{53}Fe, on the other hand, the $T'=T-\frac{1}{2}=0$ components are lower than the $T'=T+\frac{1}{2}=1$ components only for $J'<6$ and $J<\frac{15}{2}$. For $J'\geqq 6$, conversely, the $T'=0$ components become higher by about 1 MeV than the $T'=1$ components. The whole situation is presented in Fig. 3. The reason is that the p-n interactions among the $f_{7/2}$ nucleons give larger binding energies for the high-spin states of the odd-odd $N=26$ nuclei ($T'=T+\frac{1}{2}$) than they do for the high-spin states of the even-even $N=26$ nuclei ($T'=T-\frac{1}{2}$), as the number of protons is increased. Since the states with $T'=T+\frac{1}{2}$ cannot be connected to those with $T'=T-\frac{1}{2}$ by the strong $E2$ matrix elements, and since the stretched coupling states ($J'+j=J$), particularly $j=\frac{3}{2}$, play a significant role, it is difficult to obtain a $\frac{15}{2}^-$ candidate in ^{53}Fe as a member of the intruder states with a collective nature.

It has been pointed out[26] that the quadrupole-quadrupole ($Q\cdot Q$) component in the p-n interactions between the nucleons in the different shells plays an important role in the interpretation of collective phenomena in nuclei. In the weak coupling picture, the core-particle interaction may simulate such p-n interactions, and the $Q\cdot Q$ part of that interaction also plays an essential role. The matrix element of the $Q\cdot Q$ is given by

$$\langle \alpha'J',j;JM\,|\,Q\cdot Q\,|\,\overline{\alpha'J'},\overline{j};JM\rangle=(-1)^{J'+j-J}W(J'j\overline{J'}\overline{j};J2)(\alpha'J'||Q||\overline{\alpha'J'})(j||Q||\overline{j})\ .$$

This equation tells us that the two states are coupled strongly, if the quadrupole matrix elements of the cores and the particles are large. Since the $(\alpha'J'||Q||\overline{\alpha'J'})$ varies considerably from one nucleus to another and from one state to another, it governs the characteristic features of the intruder states. According to the $f^n_{7/2}$ model,[27] the $(4^+_1||Q||6^+_1)$ of ^{52}Fe is smaller by a factor of 1.5 than that of ^{50}Cr, and in ^{52}Fe the $(4^+_1||Q||6^+_2)$ is almost the same as the $(4^+_1||Q||6^+_1)$, whereas in ^{50}Cr the former matrix element is smaller by about a factor of 3 than the latter. In other words, the $(4^+_1||Q||6^+_1)$ in ^{50}Cr almost exhausts the sum $\sum_k(4^+_1||Q||6^+_k)$, while that in ^{52}Fe does not. Therefore, in ^{51}Cr $|\,^{50}\mathrm{Cr}(4^+_1)\times\nu j\rangle$ can be strongly coupled with $|\,^{50}\mathrm{Cr}(6^+_1)\times\nu j\rangle$, whereas in ^{53}Fe $|\,^{52}\mathrm{Fe}(4^+_1)\times\nu j\rangle$ can be coupled only weakly with $|\,^{52}\mathrm{Fe}(6^+_1)\times\nu j\rangle$. These $E2$ matrix elements are illustrated in Fig. 3. Considering the diagonal energies together, as discussed previously, we may suggest that there does not exist any $\frac{15}{2}^-$ candidate in ^{53}Fe as a member of the intruder states with a collective nature.

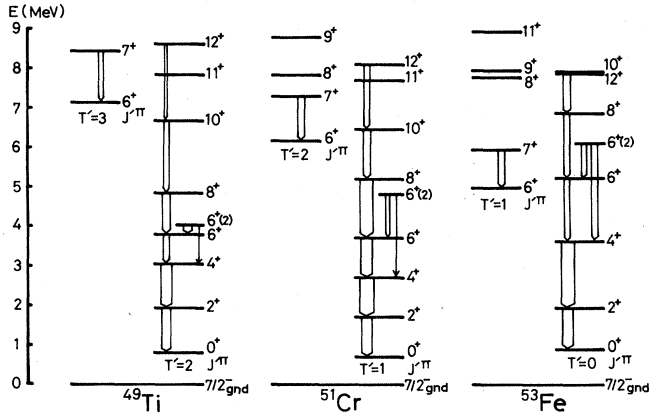

FIG. 3. Diagonal energies of the weak coupling basis states, $|\Psi(f^n_{7/2}{}^{-1}\alpha'T'J')\times p_{3/2};\alpha TJ\rangle$. The energy of the core state, $\Psi(\cdots)$, is evaluated by using the $f^n_{7/2}$ model (Ref. 27). As the core-particle interaction, we use the monopole interaction of the type $V_{ij}=a+b\mathbf{t}_i\cdot\mathbf{t}_j$. The parameters a and b are calculated with the average interaction energies of the $\langle f_{7/2}p_{3/2}\,|\,V\,|\,f_{7/2}p_{3/2}\rangle_{TJ}$ matrix elements of the effective interaction D. The single-particle energies are also taken from the fitted values. The $E2$ rates shown by the arrow are taken from the predictions by the $f^n_{7/2}$ model (Ref. 27).

IV. SUMMARY AND CONCLUSIONS

Systematic shell-model calculations of the $N\sim 28$ nuclei have been carried out within the

$$f^n_{7/2}+f^{n-1}_{7/2}(p_{3/2},p_{1/2},f_{5/2})^1$$

configurations. The effective interactions are composed partly of empirical matrix elements and partly of a phenomenological potential, and the matrix elements among the $f_{7/2}$ nucleons and the strength parameters of the potentials are determined by a least-squares fitting procedure. It is shown that the sequences of the intruder states characterized by enhanced $E2$ transitions result in ^{51}Cr and ^{53}Fe, whereas they do not appear in ^{47}Ca and ^{49}Ti. The calculated excitation energies of the low-lying intruder states are, however, systematically higher by about 0.5 MeV than the observed ones. The anomalously large $B(E2)$ values for the transitions between the low-spin intruder states in ^{51}Cr and ^{53}Fe can be reproduced very well, if the effective charges are employed from the

$2_1^+ \rightarrow 0_{gnd}^+$ $E2$ transitions of the adjacent even-even $N=26$ nuclei. The $E2$ properties of the low-lying $\frac{3}{2}^-$ states in the whole $N=27$ isotones are discussed together with the spectroscopic factors for single-neutron transfer reactions. Systematics of the $E2$ rates, including the highly hindered $E2$ transitions from the lowest $\frac{3}{2}^-$ states to the $\frac{7}{2}^-$ ground states, can be accounted for rather well by the present model. It is shown that the p-n interactions (1) among the $f_{7/2}$ nucleons and (2) between the nucleons in the $f_{7/2}$ and in the other fp shells play essential roles in the interpretation of the intruder states in the odd-mass $N=27$ isotones.

The numerical calculations were carried out with the HITAC M-200H system at the Computer Centre of the University of Tokyo.

[1]R. L. Auble, Nucl. Data Sheets **23**, 163 (1978).
[2]R. L. Auble, Nucl. Data Sheets **21**, 323 (1977); Z. P. Sawa, Phys. Scr. **7**, 5 (1973).
[3]I. M. Szöghy, J. S. Forster, and G. C. Ball, Nucl. Phys. **A201**, 433 (1973).
[4]J. Kasagi and H. Ohnuma, J. Phys. Soc. Jpn. **45**, 1099 (1978); **48**, 351 (1980); T. Kishimoto, K. Itoh, M. Sakai, J. Kasagi, and H. Ohnuma, in *Proceedings of the International Symposium on Electromagnetic Properties of Atomic Nuclei, Tokyo, 1983,* edited by H. Horie and H. Ohnuma (Tokyo Institute of Technology, Tokyo, Japan, 1983), pp. 531 and 532.
[5]A. Yokoyama, T. Oda, and H. Horie, Prog. Theor. Phys. **60**, 427 (1978).
[6]B. C. Metsch and P. W. M. Glaudemans, Nucl. Phys. **A352**, 60 (1981).
[7]I. P. Johnstone and H. G. Benson, J. Phys. G **3**, L69 (1977).
[8]J. Styczen, E. Bozek, T. Pawlat, Zb. Stachura, F. A. Beck, C. Gehringer, B. Hass, J. C. Merdinger, N. Schulz, P. Taras, M. Toulemonde, J. P. Vivien, and A. Müller-Arnke, Nucl. Phys. **A327**, 295 (1979).
[9]R. Vennink and P. W. M. Glaudemans, Z. Phys. A **294**, 241 (1980); A. G. M. van Hees and P. W. M. Glaudemans, *ibid.* **A303**, 267 (1981); R. B. M. Mooy and P. W. M. Glaudemans, *ibid.* **A312**, 59 (1983).
[10]T. T. S. Kuo and G. E. Brown, Nucl. Phys. **A114**, 241 (1968).
[11]J. B. McGrory, B. H. Wildenthal, and H. C. Halbert, Phys. Rev. C **2**, 186 (1970); S. Sharma and K. Bhatt, Phys. Rev. Lett. **30**, 620 (1973); E. A. Pasquini and A. Zuker, in *Proceedings of the European Physical Society International Conference on Nuclear Physics, Florence,* edited by P. Blasi and R. A. Ricci (Tipografia Compositori, Bologna, Italy, 1977), p. 62.
[12]H. Horie and K. Ogawa, Prog. Theor. Phys. **46**, 439 (1971).
[13]H. Horie and K. Sasaki, Prog. Theor. Phys. **25**, 475 (1961).
[14]A. H. Wapstra and N. G. Gove, Nucl. Data Tables **9**, 265 (1971).
[15]W. J. Courtney and J. D. Fox, At. Data Nucl. Data Tables **15**, 141 (1975).
[16]J. R. Beene, Nucl. Data Sheets **25**, 235 (1978).
[17]J. P. Schiffer and W. W. True, Rev. Mod. Phys. **48**, 191 (1976).
[18]M. L. Halbert, Nucl. Data Sheets **22**, 59 (1977).
[19]M. L. Halbert, Nucl. Data Sheets **24**, 175 (1978).
[20]P. A. Mandò, P. Sona, N. Tacceti, F. Brandolini, C. Rossi Alvarez, and M. De Poli, J. Phys. G **9**, 1211 (1983).
[21]P. A. Mandò, G. Poggi, P. Sona, and N. Tacceti, Phys. Rev. C **23**, 2008 (1981).
[22]W. Haar and F. W. Richter, Z. Phys. **231**, 1 (1970).
[23]K. V. K. Iyengar and B. C. Robertson, Nucl. Phys. **A174**, 385 (1971).
[24]S. Cochavi and K. Nagatani, Phys. Rev. C **4**, 2083 (1971).
[25]R. O. Nelson, C. R. Gould, D. R. Tilley, and N. R. Roberson, Nucl. Phys. **A215**, 541 (1973).
[26]K. Ogawa, Phys. Rev. C **15**, 2209 (1977).
[27]W. Kutschera, B. A. Brown, and K. Ogawa, Riv. Nuovo Cimento **1**, 1 (1978).